REVISTA MATÉRIA V.26 N.02
SSN 1517-7076 articles e12990, 2021

Mechanical property test and analysis on the main body frame structure of electrical dust precipitator

Xuewen Wang [1], Xin Zhang [1], Jiacheng Xie [1]

[1] Shanxi Key Laboratory of Fully Mechanized Coal Mining Equipment, College of Mechanical and Vehicle Engineer-ing, Taiyuan University of Technology, n.79, West Street Yingze, 030024,Taiyuan, Shanxi, P.R.China.
e-mail:wxuew@163.com, zhangxin0035@link.tyut.edu.cn, xiejiacheng@tyut.edu.cn

ABSTRACT

The objective of this work is to test the strength reserve, the working stability, the vibration performance and the dynamic response under stochastic load on the optimized main body frame structure of a type of electrical dust precipitator. The test program is established which is a test process, as well as a feedback process. The strength prototype test is carried out to study the strength reserve of the structure. Based on the mechanical model, the modal analysis, the buckling analysis, and the seismic analysis is carried out using ANSYS to study the working stability and the vibration performance of the structure. The test results show that the strength reserve of the structure is sufficient, the main body structure will not be instability in working, the structure's landscape orientation rigidity is feasible, the two-dimensional rigidity is even, and its torsional rigidity is better. The Maximum lateral displacement and stress meet the standard requirements. Obviously, the main body structure is optimized perfectly and the method is feasible that to do the performance tests after structure optimization design.

Key words: Electrical dust precipitator, Steel braced frame structures, Strength, Stability, Seismic analysis

1. INTRODUCTION

Steel braced frame structures system is constructed of shear braced steel structures and beam column steel frame [1, 2]. Beam column steel frame, which may be hinged or rigid connection, bears the vertical load transmitted by wall, beam and plate [3]. Provided by steel braced, lateral stiffness could either prevent instability of frame column or carry horizontal loads such as wind and seismic forces [4]. Formed by frame and brace, double resistance to lateral force system is a cost-effective structure type that have some characters, such as a simple structure, a big integral rigidity, good anti-seismic properties, anti-overturning properties and stability [5]. This could coordinate the mechanical performance of the frame and braced better. So steel braced frame structures system is widely used in mechanical structures and high-rise buildings, which includes a large electrical dust precipitator [6-8]. Its main braced structures is a closed self-balance, protect and spatial stress system, which consists of a wide and narrow beam on the box structure, a roof boarding, a column, mudsill, a side wall, a support beam and an ash bucket bracket, which form a particular steel braced frame structures.

There are some researches about the design and calculation of steel braced frame structures. For example, structural calculation and experimental research on strength and stiffness [9-12], buckling analysis and stability analysis [13-15], static and dynamic behavior analysis [16, 17], Seismic Analysis or Seismic Performance study [18-20], vibration characteristics [21-22], experimental study [23-26]. From the different point of view, the structural characteristics or mechanical properties of the steel frame braced structures are investigated and discussed. It could be obtained that the calculation of these structures involves many aspects, such as strength, stiffness, vibration, anti-seismic and stability, and it is difficult to obtain their mechanical and structural properties comprehensively.

A calculation and test method which could research the mechanical and structural characteristics of an optimized main support structure of the specific type large scale electrical dust precipitator is established. The mechanical and structural characteristics contain structural strength, stability, torsion effect and seismic response. Analysis and calculation methods of steel braced frame structures are also discussed. It could provide an idea for calculation and application of similar engineering problems.

Corresponding Author : Xuewen Wang Received on: 01/10/2019 Accepted on: 12/04/2020

10.1590/S1517-707620210002.1290

2. TEST AND ANALYSIS SCHEME

A main support structure of the specific type large scale electrical dust precipitator whose model technology is bad and design safety factors is relatively large, In order to reduce the cost, the author has carried on the structure finite element computation, the structure optimization and the parameter optimization, The design calculation process involves the correctness of the finite element model, the reasonableness of analysis and optimization method, the integrity of the calculation process, the safety and reliability of the calculation results, the stability and anti-seismic of the structure after optimization are need verified by experiment. So it is necessary to conduct experiment to verify the correctness of the design calculation process. Meanwhile, the test process is also a process of continuous feedback and data correction for the design calculation process, finite element model, analysis method and optimization program.

As shown in Figure.1, the experiment and test scheme are divided into 4 parts, which are prototype strength test, virtual modal test, virtual seismic test and virtual stability test. This process is both a test process and a feedback process.

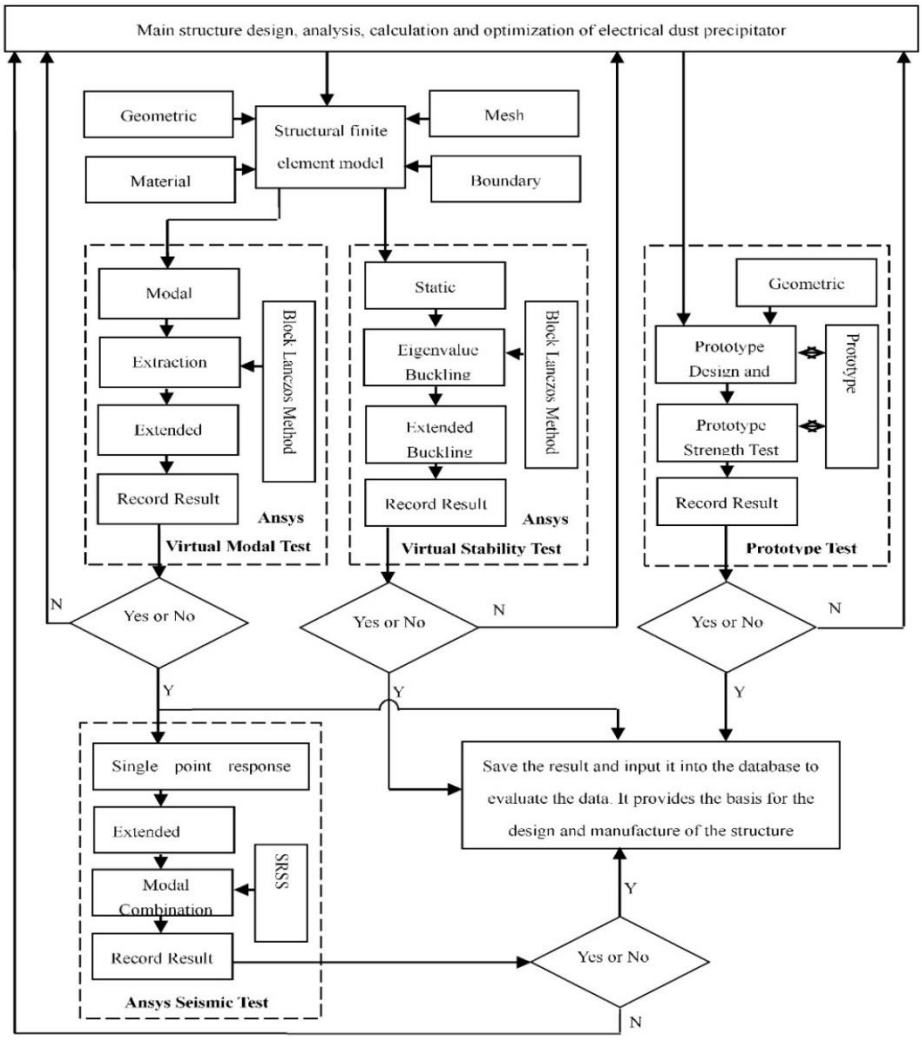

Figure 1: The test scheme.

3. MODEL

In order to realize the bearing and sealing of the electrical dust precipitator and installing and locating of other parts in their space, the main support structure of the electrical dust precipitator is a large spatial rigid frame stress system.

The optimized geometric model structure is shown in Figure 2.

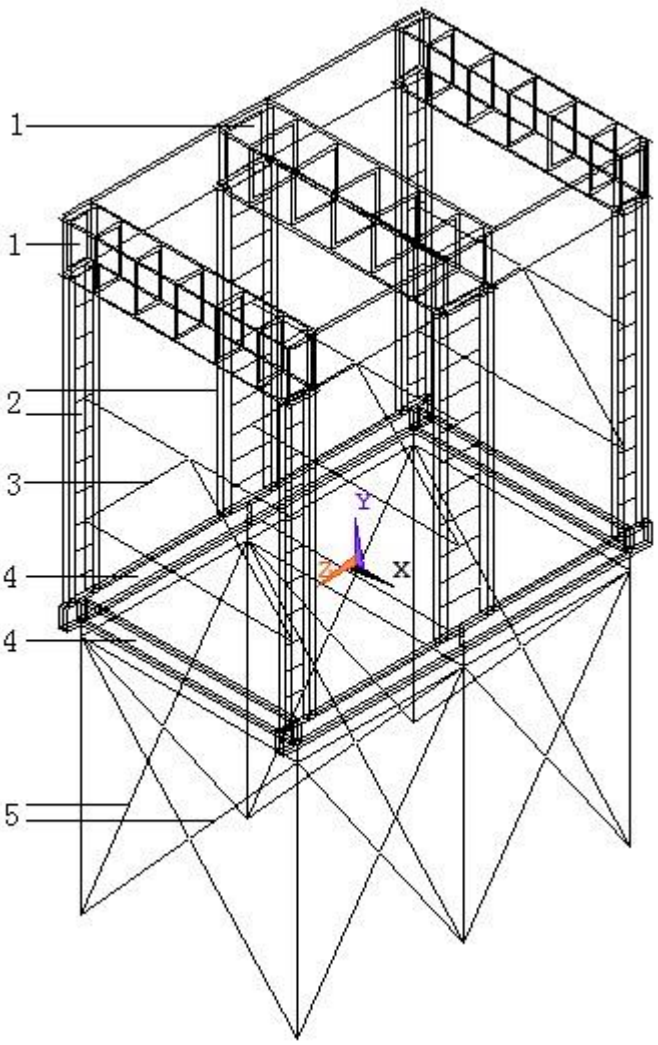

1.top beam, 2.column, 3.column support, 4.mudsill, 5.bracket

Figure 2: Geometric model after optimization of main support structure

In the process of calculation, analysis and test, shell element and the column support are integrated to simulate the some parts of the top beam, mudsill and column and the bracket and the column are equivalent to three dimensional beam element. Young modulus, density and poisson ratio are 2.1×1011Pa, 7850kg/m3, 0.3 respectively.

4. STRENGTH TEST

The optimized structure theoretically satisfies the fourth strength theory. In order to further verify the strength reserve of the optimized the structure and the rationality of the optimized method and results, it is necessary to verify strength test.

Owing to complexity of the main structure of the electrical dust precipitator, it is difficult to conduct a strength experiment on full-scale structure. This experiment also has some problems which includes wasting of manpower, material resources and financial resources, and existing some personnel safety issues. Therefore, based on the structural model test method and the principle of geometric similarity design, a text-bed is developed as the prototype of an intermediate truss girder of the main support structure, the connected force column and the force support among columns, as shown in Figure 3. The overall size of the structure is geometric similar to the actual structure and the components also conform to geometric similarity basically at the premise of satisfying the selection standard of section steel.

Table 1: The simulation test and stress test values and their comparison (stress:MPa)

MEASURING POINTS	STRESS TEST VALUES		SIMULATION TEST VALUES σ (b)	ERROR $(b-a)/b$
	MEASURED $\mu\varepsilon$	$\sigma=E\varepsilon$ (a)		
1	63	13.23	14.20	6.83%
2	144	30.24	33.00	8.36%
3	49	10.29	11.20	8.13%
4	58	12.18	14.80	17.70%
5	83	17.43	17.80	2.08%
6	40	8.40	9.30	9.68%
7	34	7.14	7.30	2.19%
8	——	——	11.50	——
9	——	——	23.00	——
10	——	——	13.30	——
11	59	12.39	13.70	9.56%
12	69	14.49	16.00	9.43%
13	67	14.07	15.60	9.81%
14	64	13.44	14.70	8.57%
15	78	16.38	17.00	3.65%
16	57	11.97	12.20	1.89%
17	62	13.02	13.10	0.61%
18	75	15.75	16.00	1.56%
19	25	5.25	5.98	12.21%
20	65	13.65	14.60	6.51%

The stress test is carried out on the test-bed (Figure 3) by the electrometric method and the results are compared with the results of finite element analysis.

The position of the strain gauge is shown in Figure 4 and the results are shown in Table 1.

Where the "measured $\mu\varepsilon$ " is a strain value (μ =10-6) read from the stress test directly, and the stress value is deduced by formula $\sigma=E\varepsilon$.

The maximum value is 30.24 MPa and the minimum value is 5.25 MPa in other measuring points. Point.6 and point.7 are slightly less than 10 MPa and the rest of the stress values are at the scope of 10MPa-20MPa.

It could be obtained that the load transferring of the optimized structure is smooth, the stress distribution is uniformity and the structure design is reasonable.

Figure 3: Test-bed

As shown in Table 1, the physical tests are basically consistent with the FEA results. Of all measurement points, seven point errors is less than 5% or slightly larger than 5%, which are basically consistent with the simulated value. Seven points error is less than 10%; two points error is larger than 10%. The error comes mainly from the following reasons.

1. Introduction;

2. Basic error of strain meter
3. Imperfection of sticking of strain gauge
4. Artificial reading error
5. Imperfection of sticking of temperature compensating piece
6. Incompletion of being constrained.
7. Reading deviation caused by the incomplete same of sticking point and the simulation point
8. Loading deviation caused by the analog loading point and the test loading points
9. The error of strain meter zero drift caused by loading shock
10. The error of loading weight

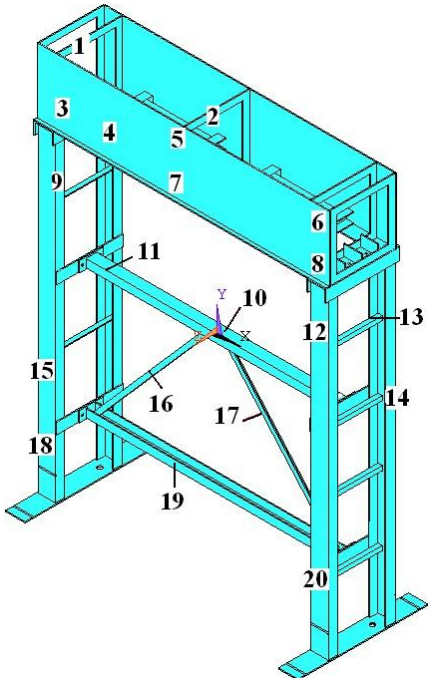

Figure 4: Strain gauge patch diagram

5. ANALYSIS OF STABILITY

It is necessary to evaluate its structural stability for the optimized main structure. Instability, also known as buckling, is that the structure loses its linear balance and transits to curve balance. Totally different in nature with strength failure, buckling appears that if the structure is unstable, the small external disturbance will increase the deformation of the structure obviously.

The main supporting structure of the electrical dust precipitator can be regarded as three main parts, which are beam, column and mudsill. Among them, the column plays a key role for stability of the main structure. Therefore, the research object of the stability test is the frame which is composed of column and column support, as shown in Figure 5.

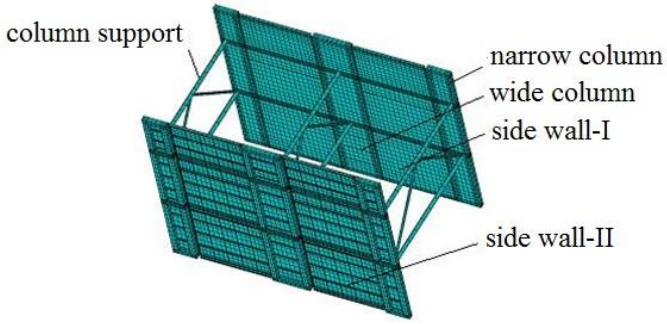

Figure 5: Geometric model for stability testing

Generally, buckling analysis of structures refers to some complex elastic (plastic) theory and mathematic calculation. To acquire the critical buckling load, it has no choice but to solve the higher order partial differential equations. And only in some conditions with simple structures, analysis key could be obtained accurately. Therefore, most of the cases are analyzed by approximate analytical methods such as energy method, numerical method and finite element method.

In this paper, in order to get the buckling load of the main supporting structure, the scale factor of the stress stiffness matrix of the main supporting structure's negative stiffness could be calculated as the eigenvalue formula based on ANSYS buckling analysis technique. The critical buckling load and the instability mode of the structure are obtained by extracting the eigenvalues of stiffness matrix of linear system, the key is to solve the following equation:

$$(K+\lambda S)\varphi = 0 \tag{1}$$

Where K is the stiffness matrix, λ is the number of eigenvalue, S is the stress stiffness matrix, φ is the displacement characteristic vector.

The discrete elastic body has n freedom degrees and it is only need to calculate the smallest eigenvalue.

The test procedure is shown in Figure 1, the buckling shapes are shown in Figure 6, Figure 7, and Figure 8 respectively.

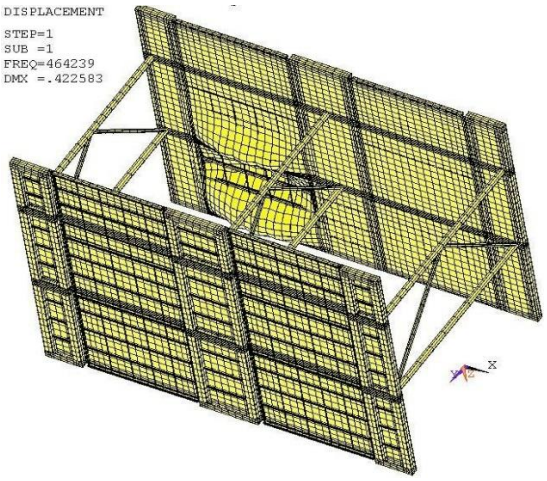

Figure 6: The first-order buckling mode

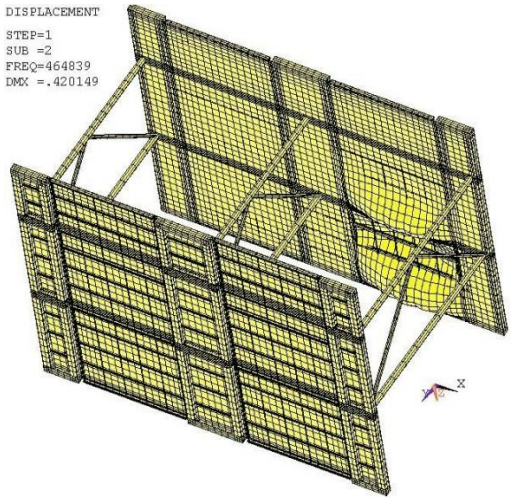

Figure 7: The second-order buckling mode

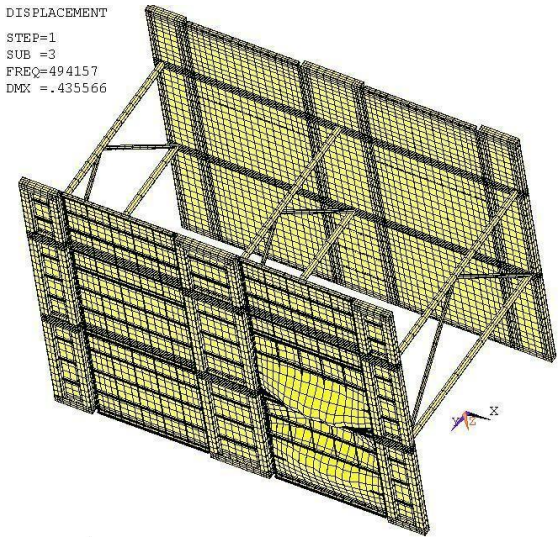

Figure 8: The third-order buckling mode

Three order buckling model value of structure is shown in Figure 9. The three order buckling loads are 464239N, 464839N, 494157N respectively, which are much larger than the working load, and could be considered that the main structure will not be instability in normal operation condition.

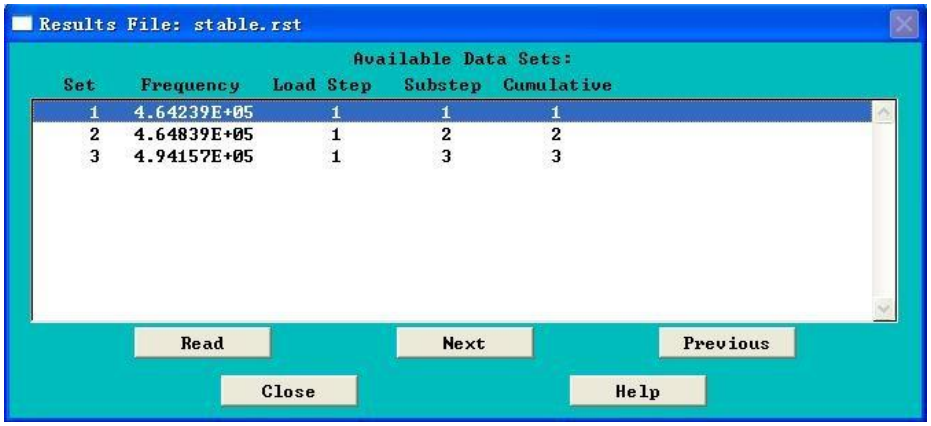

Figure 9: Three order buckling modal values of structures

6. ANALYSIS OF MODAL

The vibration characteristics of the electrical dust precipitator main structure are determined by modal analysis. The modal parameters, such as dynamic characteristics natural frequency, damping ratio and vibration, are determined to study the stiffness and torsional effect of the main supporting structure.

It is of great significance to select the correlation parameters for the results of modal analysis. The correlation parameters consist of the determination of exciting frequency, the avoidance and utilization of resonance phenomena. It could also provide a research starting point for further dynamic analysis. In this paper, the spectral analysis of seismic response of the main supporting structure is based on the modal analysis, as shown in Figure 1.

The basic idea of modal analysis is to decouple the matrix equation which describes the dynamic behavior of machinery and structures, so the dynamic characteristics of the freedom system with N degree could be expressed by the freedom system with a single degree. It is a typical method for solving eigenvalue problems.

$$[K]\{\phi_i\} = \omega_i^2 [M]\{\phi_i\} \tag{2}$$

Where $[K]$ is the stiffness matrix, $\{\phi_i\}$ is the characteristic vibration mode vector of No.i order mode, ω_i is the natural frequency of No.i order mode, $[M]$ is the mass matrix.

Analysis procedures and methods are shown in Figure 1 and Table 2 lists the frequencies, periods and

vibration mode characteristics of the first four orders modes.

The first natural vibration period of the structure is 1.8248s, which is a small value, and indicates that the lateral stiffness is relatively reasonable. Approximate equality of the vertical period and the horizontal period indicate that the plane stiffness of the structure is uniform, the anti-seismic performance is good. T3/T1=0.4388, It could be obtained obviously that the first natural vibration period which mainly appear torsion is moderate and the torsional effect is not very obvious.

Table 2: The first four natural frequencies of the main support structure

ORDERS	FREQUENCY- f(s-1)	PERIOD- T(s)	MODE OF VIBRATION
1	0.5480	1.8248	Lateral motion dominates
2	0.6760	1.4793	Vertical motion domina
3	1.2488	0.8008	Torsional vibration
4	1.5089	0.6627	Localized vibration

7. ANALYSIS OF SEISMIC

The main body structure of the electrical dust precipitator is a frame type support structure of house shape and has some characters, which contain (relative high of the running state center of gravity, relative long of the natural vibration period, resonating with the seismic wave easy.) Therefore, it is necessary to study the dynamic response of the optimized structure under random load. In this paper, the modal analysis method [27-28] is used to calculate the seismic response of the structure by combining the modal analysis results with a known spectrum.

7.1 Design of response spectrum

There are many methods of seismic analysis and anti-seismic design, of which the method most widely used is the response spectrum theory, which is proposed by Biot firstly [29]. The so-called spectrum is the relationship between the spectral value and frequency and reflects the strength and frequency of the time-process load. The core of the elastic response spectrum theory is the response spectrum curve. The so-called response spectrum is the curve of the maximum response of a single point system with the period of self-earthquake under a given ground motion.

According to the different properties of the reaction, there are some different displacement response spectrum, such as the velocity response spectrum and the acceleration response spectrum. Generally, it is necessary to determine the magnitude of seismic forces which is acting on the structure and is caused by the ground motion, then check the structural strength and deformation. For anti-seismic analysis, Therefore, the acceleration response spectrum are the main parameters which reflects the seismic action in the linear anti-seismic design criterion [30, 31].

The definition of the acceleration response spectrum is the curve of the maximum absolute acceleration response of a single point system with the period of natural vibration under the effect of a given ground motion. The procedure of designing the standard acceleration response spectrum is as following: drawing and classifying the spectral curves according to the previous strong earthquake records were in accordance with the magnitude and site conditions, and were statistically averaged, get a set of representative curves, then make a smooth processing and moderate adjustment.

Under the effect of the action of horizontal ground motion, the absolute acceleration of a single mass point system of mass m is $a(t)$, the mass point suffered by horizontal seismic action is:

$$F(t) = m\alpha(t) \tag{3}$$

The formula (3) indicates that the magnitude and direction of the mass point horizontal seismic action change with time t during the earthquake. The maximum value of seismic action is usually used in anti-seismic analysis, its value can be expressed as:

$$F = m\alpha_{\max} = (W / g)\alpha_{\max} = \alpha W \tag{4}$$

Where g is gravity acceleration, $\alpha = \alpha_{max} / g$ is the seismic influence coefficient, which is the maximum absolute acceleration of a mass point in a gravitational acceleration g with the single mass point elastic system under the action of earthquake.

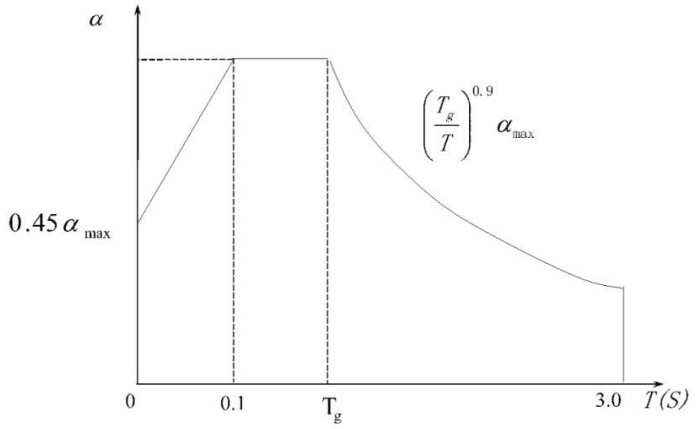

Figure 10: Influence coefficient α curve of seismic α-seismic influence coefficient, α_{max} - maximum earthquake influence coefficient, T - natural vibration period of structure, T_g- characteristic period

$$\alpha = \frac{\alpha_{max}}{g} = \frac{|\ddot{x}_g|_{max}}{g} \frac{\alpha_{max}}{|\ddot{x}_g|_{max}} = K\beta \tag{5}$$

α Depends on fortification intensity or basic intensity, seismic geological environment (source distribution, seismic series, epicentral distance and propagation path, etc.) and site condition. According to the domestic and foreign hundreds of earthquake response spectrum analysis, Chinese scholars have established the relation curve $\alpha(T)$ between the seismic influence coefficient α and the natural vibration period T of the structural system. As shown in Figure 10 [32].

Table 3: The value of $T_g(s)$

	FIELD I	FIELD II	FIELD III	FIELD IV
Near-seismic	0.2	0.3	0.4	0.65
Tele-seismic	0.25	0.45	0.55	0.85

Table 4: The value of α_{max}

Seismic intensity	7	8	9
α_{max}	0.08	0.16	0.32

The choice of α_{max} and $T_g(s)$ is shown in Table 3 and Table 4.

Table 3 field types are divided into four parts, which are hard field I, medium hard field II, soft field III and weak field IV.

Table 5: The seismic response spectrum

Frequency- f(s-1)	0.5480	0.6760	1.2488	1.5089	1.7700	2.024
Period- T(s)	1.8278	1.4793	0.8008	0.6627	0.5650	0.4941
α	0.0158	0.0190	0.0331	0.0392	0.0453	0.0511
Frequency- f(s-1)	2.1395	2.3704	2.4375	2.6003	2.7410	2.8256
Period- T(s)	0.4674	0.4219	0.4103	0.3846	0.3648	0.3539
α	0.0537	0.0589	0.0604	0.0640	0.0671	0.0689
Frequency- f(s-1)	2.9771	3.1434	3.7460	4.2316	10.0000	1000.0000
Period- T(s)	0.3365	0.3181	0.2670	0.2363	0.1000	0.0010

α	0.0723	0.0759	0.0800	0.0800	0.0800	0.0360

A type of electrical dust precipitator installed in the II site, under the condition of seven level near source seismic loading, according to Table 3 and Table 4, Tg =0.3, α_{max} =0.08.

It could be obtained from Figure 10 that the corresponding coefficient equation of the earthquake is as follows:

$$\begin{cases} \alpha = \left[\dfrac{0.08*(1-0.44)}{0.1}\right]T + 0.08\times 0.45 & 0 < T \le 0.1 \\ \alpha = 0.08 & 0.1 < T \le 0.3 \\ \alpha = (0.3/T)^{0.9}\times 0.08 & 0.3 < T \le 3 \end{cases} \tag{6}$$

According to the formula (6), the seismic response spectrum is shown in Table 5. The response spectrum analysis is the analysis in frequency domain and the response of the structure is related to the width of the frequency domain. The selected response spectrum in Table 5 guarantee a certain width frequency domain and the finite vibration frequency range of cover main structure.

7.2 Results analysis

According to the response spectrum theory, the multi-degree of freedom system could be decomposed into several generalized (equivalent) single degree of freedom systems. The maximum seismic response of each generalized equivalent single degree freedom system is equal to the maximum seismic response of each equivalent single degree freedom system. Therefore, ANSYS could be used for single point response spectrum analysis, take g =9.82, based on the assumption that the structure is rigid and the seismic effect of support is identical, horizontal and vertical have been motivated simultaneously, SRSS method is used to carry on vibration modal combination, the comprehensive reaction have been obtained by square and square root of seismic effect of each order, as shown in formula (7):

$$\overline{Q} = \sqrt{\sum \overline{Q_i}} \tag{7}$$

Where $\overline{Q}$ means total response of the system, $\overline{Q_i}$ represents response of i order mode

As shown in Figure 11, the maximum displacement of the structure under seismic load appears in the combination of the middle beam and the column in the direction of X, the maximum displacement is 0.031659m, the deformation is small. The maximum shear stress of XY, YZ and XZ are 2.34 MPa, 18.84 MPa and 8.14 MPa respectively. The maximum seismic stress of the structure is not on the supporting structure of the main structure, all appear in the top beam or column connection between the local steel plate, but they are less than the material strength, under the action of seismic parameters, the structure works in the elastic state.

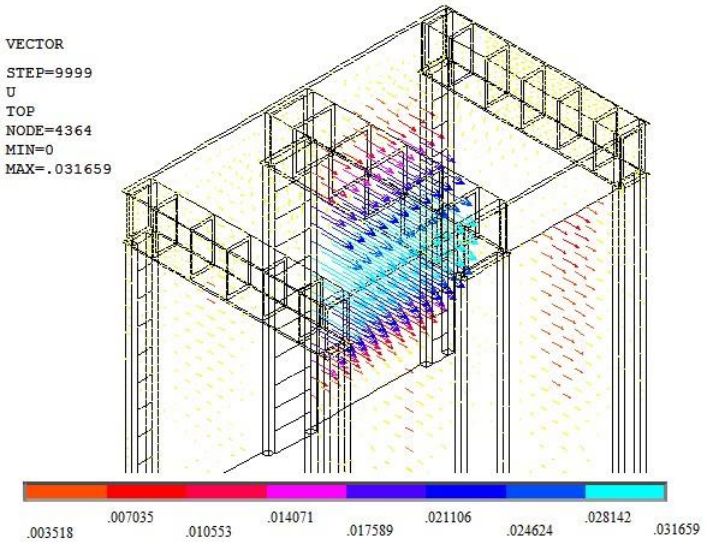

Figure 11: The seismic displacement vectors.

It should be noted that the response spectrum analysis method consider the influence of the amplitude and frequency spectrum of seismic wave on the structure, the result is the maximum inertia force in the earthquake, and sometimes it is not necessarily the most dangerous state of the structure, If the influence of the earthquake duration on the structure and the weak link of the structure are determined, the time history analysis of the optimal structure could be considered [33-36].

8. CONCLUSION

Taking the main supporting structure of electrical dust precipitator as an object, the design and calculation methods which refer to a kind of steel braced frame structures are discussed in this paper and draw the following conclusions:

(1) The strength test shows that the main supporting structure of a certain type of electrical dust precipitator has the advantages of transferring load smoothly, uniform stress distribution and reasonable structure optimization. The buckling analysis shows that the main body structure does not produce lateral torsional instability in the working state. Modal analysis shows that the lateral stiffness of the main structure is reasonable, the plane stiffness is uniform, and the torsional stiffness is good. The response spectrum analysis shows that the maximum lateral displacement of the structure is the combination of the top of middle beam and column, the maximum lateral displacement meets the requirements, and the deformation of the other parts is continuous. The effect on the structure by the earthquake motion stress is not obvious, which shows that the anti-seismic performance of optimized structure is good under the near source seismic load of level 7 seismic intensity and field II.

(2) The above results show that the optimized main supporting structure of a certain type of electrostatic dust precipitator could meet the requirements of the strength reserve, stability and vibration.

(3) This scheme that firstly the structural optimization design is carried out and then the strength, stability and vibration are tested, is feasible for the design, calculation and analysis of large steel braced frame structure. This proposed method could provide a solution for the calculation and application of similar engineering problems.

9. ACKNOWLEDGEMENTS

This project was supported by The Merit Funding for the Returned Overseas Personnel Sci-Tech Activities, Shanxi Province, China (2016), Shanxi Scholarship Council of China (2016-043), Program for the Outstanding Innovative Teams of Higher Learning Institutions of Shanxi (2014) and the Basic Condition Platform Project of Shanxi (2014091016).

10. BIBLIOGRAPHY

[1] BUYUKTASKIN, A.H.A., "A study on the comparison of a steel building with braced frames and with RC walls", *Earthquakes and Structures*, v. 12, n.3, pp.263-270, Mar.2017.

[2] GRAY, M.G., CHRISTOPOULOS, C., PACKER, J.A., "Design and full-scale testing of a cast steel yielding brace system in a braced frame", *Journal of Structural Engineering*, v.143, n.4, pp.04016210.1-04016210.9, Nov.2016.

[3] GHODS, S., KHEYRODDIN, A., NAZERYAN, M., "Nonlinear behavior of connections in RCS frames with bracing and steel plate shear wall", *Steel and Composite Structures*, v. 22, n.4, pp. 915-935, Nov.2016.

[4] QIAO, S., HAN, X., ZHOU, K., "Conceptual configuration and seismic performance of high-rise steel braced frame", *Steel and Composite Structures*, v.23, n.2, pp. 173-186, Feb.2017.

[5] TOUTANT, G., MINOUEI, Y.B., IMANPOUR, A., *et al.*, "Stability of steel columns in steel concentrically braced frames subjected to seismic loading", In: *Structures Congress 2017: Buildings and Special Structures*, pp.65-13, Denver, Colorado, USA, April 2017.

[6] KHERBOUCHE, F., BENMIMOUN, Y., TILMATINE, A., "Study of a new electrostatic precipitator with asymmetrical wire-to-cylinder configuration for cement particles collection", *Journal of Electrostatics*, v.83, pp.7-15, Oct.2017.

[7] JI, J., DING, X., "Stiffener layout optimization of inlet structure for electrostatic precipitator by improved adaptive growth method", *Advances in Mechanical Engineering*, v.6, pp1-8, Nov.2014.

[8] ADHAV, R.S., SAMAD, A., KENYERY, F., "Optimal designs of an ESP to handle up to 10% GVF", *International Journal of Oil Gas and Coal Technology*, v.13, n.4, pp.338-358, Jan.2016.

[9] LIU, X., ZHANG, A., MA, J., *et al.*, "Design and model test of a modularized prefabricated steel frame structure with inclined braces", *Advances in Materials Science and Engineering*, v.2015, n.5, pp.1-12,

Oct.2015.
[10] TAJAMMOLIAN, H., MOFID, M., "On the characteristics and design of yielding elements used in steel-braced framed structures", *Structural Design of Tall and Special Buildings*, v.22, n.2, pp.179-191, Feb.2013.
[11] SOO, KIM HO. "Stiffness-based optimal design of tall steel braced frame structure for dynamic lateral drift control", *Journal of the Architectural Institute of Korea Structure & Construction*, v.23, n.10, pp.75-82, Oct.2007.
[12] PARK, M.H., KIM, K.W., LEE, S.J., *et al.*, "Optimum design of braced steel framed structures considering soil condition under earthquake loads", *Journal of the Korea Institute for Structural Maintenance and Inspection*, v.10, n.4, pp. 97-107, May. 2006.
[13] TONG, G., PI, Y., BRADFORD, M., "Buckling failure of an unusual braced steel frame supporting an electric dust-catcher", *Engineering Failure Analysis*, v.16, n.7, pp.2400-2407, Mar. 2009,
[14] ZHANG, L., TONG, G.S., JI, Y, "Buckling of flexural-shear bracing system and its braced steel frames", *Advances in Structural Engineering*, v.18, n.11, pp.1831-1844, Nov.2016.
[15] YIGITSOY, G., TOPKAYA, C., OKAZAKI, T., "Stability of Beams in Steel Eccentrically Braced Frames", *Journal of Constructional Steel Research*, v.96, pp.14-25, May. 2014.
[16] ESKANDARI, R., VAFAEI, D., VAFAEI, J., "Nonlinear static and dynamic behavior of reinforced concrete steel-braced frames", Earthquakes and Structures, v.12, n.2, pp.191-200, Feb. 2017.
[17] STEELE, T.C., WIEBE, L.D.A, "Dynamic and equivalent static procedures for capacity design of controlled rocking steel braced frames", *Earthquake Engineering & Structural Dynamics*, v.45, n.14, pp.2349-2369, Nov.2016.
[18] BALAZADEH-MINOUEI, Y., KOBOEVIC, S., Tremblay, R., "Seismic evaluation of a steel braced frame using NBCC and ASCE 41", *Journal of Constructional Steel Research*, v.135, pp.110-124, Jan.2017.
[19] IMANPOUR, A., TREMBLAY, R., DAVARAN, A., "seismic performance assessment of multitiered steel concentrically braced frames designed in accordance with the 2010 AISC seismic provisions", *Journal of Structural Engineering*, v.143, n.5, pp.1-13, Dec.2016.
[20] MAZZOTTA, V., BRUNESI, E., NASCIMBENE, R., "Numerical modeling and seismic analysis of tall steel buildings with braced frame systems", *Periodica Polytechnica Civil Engineering*, v. 61, n.2, pp.196-208, Mar.2017.
[21] LEE, H., "A vibration response analysis of steel building frame with k shape brace vibrationally controlled by turbulent flow dampers sealed by viscoelastic material", *Journal of the Korean Association for and Spatial Structures*, v.2, n.20, pp. 61-68, Jan.2006.
[22] TREMBLAY, R., "Fundamental periods of vibration of braced steel frames for seismic design", *Earthquake Spectra*, v.21, n.3, pp.833-860, Aug. 2005.
[23] SU, M., LIAN, M., GUO, Y., "Experimental performance of y-shaped eccentrically braced frames fabricated with high strength steel", *Steel and Composite Structures - An International Journal*, v.24, n.4, pp.441-453, Jul. 2017.
[24] ZHANG, J., WU, B., MEI, Y., "Experimental and analytical studies on a reinforced concrete frame retrofitted with buckling-restrained brace and steel caging", *Advances in Structural Engineering*, v.18, n.2, pp.155-171, Feb.2015.
[25] GRAY, M.G., CHRISTOPOULOS, C., PACKER, J.A., "Cast steel yielding brace system for concentrically braced frames: concept development and experimental validations", *Journal of Structural Engineering*, v.140, n.4, pp.1-11, Apr. 2014.
[26] METELLI, G., "Theoretical and experimental study on the cyclic behaviour of X braced steel frames", *Engineering Structures*, v.46, pp.763-,773, Aug.2013.
[27] KIM, T., PARK, I., LEE, U., "Forced vibration of a timoshenko beam subjected to stationary and moving loads using the modal analysis method", *Shock and Vibration*, v.2017, n.5, pp.1-26, Jan.2017.
[28] PAN, W., TANG, G., ZHANG, M., "Modal analysis method for blisks based on three-dimensional blade and two-dimensional axisymmetric disk finite element model", *Journal of Engineering for Gas Turbines and Power-Transactions of the Asme*, v.139, n.5, pp.1-12, May.2017.
[29] Biot, M.A, "A mechanical analyzer for perdition of earthquake stress", *Seismological Research Letters*, v.31, n.1, pp.151- 171, May.1941.
[30] RUANGRASSAMEE, A., PALASRI, C., LUKKUNAPRASIT, P., "Bi-Directional Pseudo-Acceleration response spectra", *Journal of Earthquake and Tsunami*, v.10, n.4, pp.1650007, Mar.2016.
[31] CHEN, J., WANG, L., RACIC, V., "Acceleration response spectrum for prediction of structural vibration due to individual bouncing", *Mechanical Systems and Signal Processing*, v.76-77, pp. 394-408, Aug.2016.
[32] CAO, Y., *The 3-D Simulation of Tall Building with Frame Structu*re, Tese de Sc, Taiyuan University of Technology, Taiyuan, China,2005
[33] LEE, D.H., KIM, B. H., JEONG, S.H., "Seismic fragility analysis of a buried gas pipeline based on non-

linear time-history analysis", *International Journal of Steel Structures*, v.16, n.1, pp.231-242, Mar.2016.
[34] DE A. A., PECCE, M., ROSSI, F., "Linear time history analysis for the out-of-plane seismic demand of infill walls in rc framed buildings", *Bulletin of Earthquake Engineering*, v.13, n.11, pp.3325-3352, Nov.2015.
[35] ORMENO, M., LARKIN, T., CHOUW, N., "Evaluation of seismic ground motion scaling procedures for linear time-history analysis of liquid storage tanks", *Engineering Structures*, v.102, pp.266-277, Aug.2015.
[36] DONG, D., LI, J., TENG, Y., "Anti-seismic device design for container crane and its elastic-plastic time history analysis", *Polish Maritime Research*, v.22, pp.30-34, Sep.2015.

ORCID
Xuewen Wang https://orcid.org/0000-0001-6028-9430
Xin Zhang https://orcid.org/0000-0002-9936-8600
Jiacheng Xie https://orcid.org/0000-0002-7136-1140